

Cobalt(III) Bis-*o*-semiquinone Complexes with *p*-Tolyl-Substituted Formazan Ligands: Synthesis, Structure, and Magnetic Properties

N. A. Protasenko^{a,*}, E. V. Baranov^a, I. A. Yakushev^b, A. S. Bogomyakov^c, and V. K. Cherkasov^a

^a Razuvaev Institute of Organometallic Chemistry, Russian Academy of Sciences, Nizhny Novgorod, Russia

^b Kurnakov Institute of General and Inorganic Chemistry, Russian Academy of Sciences, Moscow, Russia

^c International Tomography Center, Siberian Branch, Russian Academy of Sciences, Novosibirsk, Russia

*e-mail: nprotasenko@iomc.ras.ru

Received April 19, 2022; revised May 13, 2022; accepted May 17, 2022

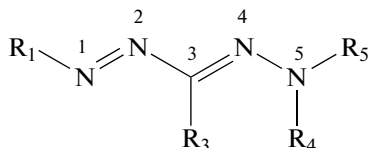
Abstract—New heteroligand cobalt(III) bis-3,6-di-*tert*-butyl-*o*-benzosemiquinone complexes with *p*-tolyl-substituted formazan ligands $\text{Co}(3,6\text{-SQ})_2\text{L}^n$ (L^1H is 1,5-diphenyl-3-*p*-tolylformazan (**I**), L^2H is 1,3,5-tri-*p*-tolylformazan (**II**), and L^3H is 3-nitro-1,5-di-*p*-tolylformazan (**III**)) are synthesized and characterized. The molecular structures of compounds **I**, **II**, and **III** in the crystalline state are determined by X-ray diffraction (XRD) (CIF files CCDC nos. 2161722 (**I**), 2167094 (**II**), and 2167095 (**III**)). According to the XRD results and magnetic and spectral measurement data, compounds **I–III** are complexes of low-spin cobalt(III) bound to two radical anion *o*-semiquinone ligands and one formazan anion. The magnetic behavior of the complexes in a temperature range of 2–300 K is characterized by intramolecular antiferromagnetic exchange interactions between the *o*-semiquinone ligands. The replacement of the phenyl substituents by *p*-tolyl groups in positions 1 and 5 of the diamagnetic formazanate ligand results in a significant enhancement of the exchange between the radical centers.

Keywords: cobalt(III) complexes, *o*-semiquinone, formazan, XRD, magnetochemistry

DOI: 10.1134/S1070328422700129

INTRODUCTION

Compounds containing the azohydrazone system of bonds with the general formula



are named formazans.

1,3,5-Trisubstituted formazans are studied to a highest extent. In the chemistry of formazans, substituents at the N(1) and N(5) nitrogen atoms are traditionally designated as R^1 and R^5 , and a substituent at the carbon atom in position 3 is designated as R^3 . Compounds of the formazan class are widely used as ligands in coordination chemistry due to simplicity of their synthesis, a mobile π system, conformational flexibility, and interesting redox properties [1, 2]. The metal complexes of formazans are presently studied intensively because of a possibility of using in catalysis [3, 4] and design of molecular magnets [5–7]. In addition, the formazanate complexes based on boron difluoride (BF_2) have unique optoelectronic properties and turned out to be good fluorescent agents for

cell visualization [8, 9], electrochemiluminescence emitters [10, 11], and building blocks for polyfunctional polymers [12, 13]. Formazan ligands can also be used for the preparation of heteroligand metal complexes. Coordination compounds of this type containing ligands of various nature demonstrate more possibilities for controlling their redox and optical properties by the variation of the metal ion of the complexing agent, substituents in the formazanate chain, and nature of additional ligands [14–19].

Our research group is interested in studies of the heteroligand metal complexes containing the radical redox-active *o*-quinone-based ligands and diverse N-donor ligands [20–22]. We have previously synthesized and characterized the first examples of the cobalt complexes bearing simultaneously redox-active ligands of two types: *o*-quinone and formazanate [23, 24]. The influence of electron-acceptor groups in position 3 of the formazanate ligand on the magnetic and electrochemical behavior of the heteroligand cobalt *o*-semiquinoneformazanate complexes was studied [25].

The results of the synthesis and spectral, magnetic, and structural studies of three new cobalt(III) bis-*o*-semiquinone complexes with the *p*-tolyl-substituted formazan ligands are presented in this work.

EXPERIMENTAL

3,6-Di-*tert*-butyl-*o*-benzoquinone [26], 1,5-diphenyl-3-*p*-tolylformazan [27], 1,3,5-tri-*p*-tolylformazan [27], 3-nitro-1,5-di-*p*-tolylformazan [28], and tris(3,6-di-*tert*-butyl-*o*-benzosemiquinolone)cobalt(III) [29] were synthesized according to known procedures. The solvents necessary for experiments were purified and dehydrated according to standard procedures [30].

IR spectra were recorded on an FSN-1201 FT-IR spectrometer (400–4000 cm⁻¹, Nujol). Elemental analysis (C, H, N) was carried out on an Elementar Vario EL cube elemental analyzer. Magnetochemical measurements were carried out at the International Tomography Center (Siberian Branch, Russian Academy of Sciences) on an MPMSXL SQUID magnetometer (Quantum Design) in a range of 2–310 K in a magnetic field of 5 kOe. The paramagnetic components χ were determined taking into account the diamagnetic contribution estimated from Pascal's constants. The effective magnetic moment (μ_{eff}) was calculated by the equation $\mu_{\text{eff}} = [3k\chi T / (N_A \mu_B^2)]^{1/2}$, where N_A , μ_B , and k are Avogadro's number, Bohr magneton, and Boltzmann constant, respectively.

Synthesis of complex Co(3,6-SQ)₂L¹ (I). A solution of 1,5-diphenyl-3-*p*-tolylformazan (0.031 g, 0.1 mmol) in toluene (5 mL) was poured to a solution of tris(3,6-di-*tert*-butyl-*o*-benzosemiquinolone)cobalt(III) (0.070 g, 0.1 mmol) in toluene (10 mL). The reaction mixture was stirred at room temperature for 24 h. The solution turned dark blue. Then the most part of the solvent was evaporated, and hexane (10 mL) was added. The resulting solution was held at 4°C in a refrigerator for 14 h. As a result, fine dark blue prismatic crystals were formed, filtered off, and dried in vacuo (80% yield).

For C₄₈H₅₇N₄O₄Co

Anal. calcd., %	C, 70.92	H, 7.07	N, 6.89
Found, %	C, 70.79	H, 7.35	N, 6.82

IR (ν, cm⁻¹): 1659 w, 1592 w, 1550 m, 1515 m, 1484 s, 1451 s, 1427 s, 1388 m, 1357 s, 1335 s, 1305 s, 1276 s, 1194 s, 1153 w, 1110 w, 1078 w, 1026 m, 995 m, 974 s, 955 s, 910 w, 894 w, 829 s, 822 s, 807 w, 781 m, 761 s, 692 s, 667 m, 652 m, 620 w, 580 w, 532 m, 523 w, 503 w, 486 m, 474 w.

Synthesis of complexes Co(3,6-SQ)₂L² (II) and Co(3,6-SQ)₂L³ (III). Complexes II and III were synthesized using a procedure analogous to that described for complex I.

For complex II: dark blue prismatic crystals crystallized from hexane (86% yield).

For C₅₀H₆₁CoN₄O₄

Anal. calcd., %	C, 71.41	H, 7.31	N, 6.66
Found, %	C, 71.25	H, 7.61	N, 6.73

IR (ν, cm⁻¹): 1661 w, 1610 w, 1599 m, 1562 w, 1553 m, 1503 w, 1433 s, 1390 s, 1359 m, 1348 s, 1305 w, 1287 w, 1279 m, 1210 m, 1200 w, 1183 w, 1112 w, 1029 m, 978 s, 960 s, 830 s, 782 w, 762 m, 689 m, 649 s, 622 w, 577 s, 507 m, 498 s.

For complex III: brown prismatic crystals crystallized from pentane (81% yield).

For C₄₃H₅₄CoN₅O₆

Anal. calcd., %	C, 64.89	H, 6.84	N, 8.80
Found, %	C, 64.74	H, 6.91	N, 8.95

IR (ν, cm⁻¹): 1681 s, 1655 s, 1603 w, 1583 w, 1547 w, 1525 m, 1502 w, 1481 s, 1427 s, 1413 m, 1360 s, 1287 s, 1209 w, 1197 m, 1168 w, 1140 w, 1111 w, 1024 w, 1015 w, 975 m, 958 m, 939 s, 923 m, 898 m, 869 w, 841 w, 824 s, 813 m, 801 m, 784 w, 752 w, 734 w, 721 w, 693 w, 650 s, 641 m, 578 w, 548 w, 529 w, 504 w, 483 m.

XRD. The XRD data for a single crystal of complex I were obtained on a Bruker D8 Venture Photon diffractometer in the φ and ω scan modes at the Center for Collective Use of the Kurnakov Institute of General and Inorganic Chemistry (Russian Academy of Sciences) at 100 K ($\lambda(\text{CuK}\alpha) = 1.54178 \text{ \AA}$, Incoatec I μ S 3.0 microfocus X-ray radiation source). The initial indexing was performed, unit cell parameters were refined, and reflections were integrated using the Bruker APEX3 program package [31]. An absorption correction of reflection intensities was applied using the SADABS program [31]. The structure was solved by direct methods [32] and refined by full-matrix least squares for F^2 [33] in the anisotropic approximation for all non-hydrogen atoms without restraints on thermal or geometric parameters of the model. Hydrogen atoms were placed in the calculated positions and refined by the riding model with $U_{\text{iso}}(\text{H}) = 1.5U_{\text{equiv}}(\text{C})$ for the hydrogen atoms of the methyl groups and $U_{\text{iso}}(\text{H}) = 1.2U_{\text{equiv}}(\text{C})$ for other hydrogen atoms. The calculations were performed using the SHELXTL software [33] in the OLEX2 program of structural data visualization and processing [34].

The XRD data for compounds II and III were collected on Agilent Xcalibur E and Bruker D8 Quest single-crystal diffractometers, respectively (MoK α radiation, $\lambda = 0.71073 \text{ \AA}$, φ and ω scan modes). Diffraction data were collected, initial reflection indexing was performed, and unit cell parameters were refined using the CrysAlisPro (for II) [35] and APEX3 (for

Table 1. Crystallographic data and experimental and structure refinement parameters for compounds **I–III**

Parameter	Value		
	I	II	III
Empirical formula	C ₄₈ H ₅₇ CoN ₄ O ₄	C ₅₀ H ₆₁ CoN ₄ O ₄	C ₄₈ H ₆₆ CoN ₅ O ₆
<i>FW</i>	812.90	840.95	867.98
<i>T</i> , K	100(2)	298(2)	100(2)
Crystal system	Monoclinic	Triclinic	Monoclinic
Space group	<i>P</i> 2 ₁ / <i>c</i>	<i>P</i> $\bar{1}$	<i>P</i> 2 ₁ / <i>c</i>
<i>a</i> , Å	10.1605(6)	11.0609(3)	14.2129(5)
<i>b</i> , Å	38.045(2)	11.5215(2)	30.4541(10)
<i>c</i> , Å	11.1911(6)	19.4051(4)	11.1943(4)
α , deg	90	101.827(2)	90
β , deg	100.840(4)	103.185(2)	100.116(1)
γ , deg	90	94.836(2)	90
<i>V</i> , Å ³	4248.8(4)	2334.25(9)	4770.0(3)
<i>Z</i>	4	2	4
ρ_{calc} , mg/m ³	1.271	1.196	1.209
μ , mm ⁻¹	3.546	0.414	0.411
θ , deg	2.32–67.00	2.44–25.03	2.24–28.00
Number of observed reflections	38299	32772	62753
Number of independent reflections	7439	8244	11482
<i>R</i> _{int}	0.1656	0.0330	0.0433
<i>S</i> (<i>F</i> ²)	0.986	1.004	1.072
<i>R</i> ₁ , <i>wR</i> ₂ (<i>I</i> > 2σ(<i>I</i>))	0.0714, 0.1519	0.0462, 0.1065	0.0518, 0.1244
<i>R</i> ₁ , <i>wR</i> ₂ (for all parameters)	0.1426, 0.1861	0.0755, 0.1222	0.0584, 0.1272
$\Delta\rho_{\text{max}}/\Delta\rho_{\text{min}}$, e Å ⁻³	0.369/–0.691	0.341/–0.314	1.732/–0.540

III) program packages [36]. Experimental sets of intensities were integrated using the CrysAlisPro (for **II**) [35] and SAINT (for **III**) program packages [37, 38]. The structures of compounds **II** and **III** were solved by direct methods using the dual-space algorithm in the SHELXT program [32] and refined by full-matrix least squares for F_{hkl}^2 in the anisotropic approximation for nonhydrogen atoms. Hydrogen atoms were placed in the geometrically calculated positions and refined isotropically. The structures were solved using the SHELXTL software [33, 39]. An absorption correction was applied in the SCALE3 ABSPACK [40] and SADABS [41] programs for compounds **II** and **III**, respectively. In a molecule of complex **II**, the *p*-tolyl substituent at the N(1) atom was disordered over two positions. The solvate *n*-pentane molecule in the general position was found in the crystal of compound **III**. The ratio of molecules of the *n*-pentane and cobalt complex was 1 : 1.

The crystallographic data and structure refinement parameters for complexes **I**, **II**, and **III** are given in Table 1. Selected bond lengths are listed in Table 2.

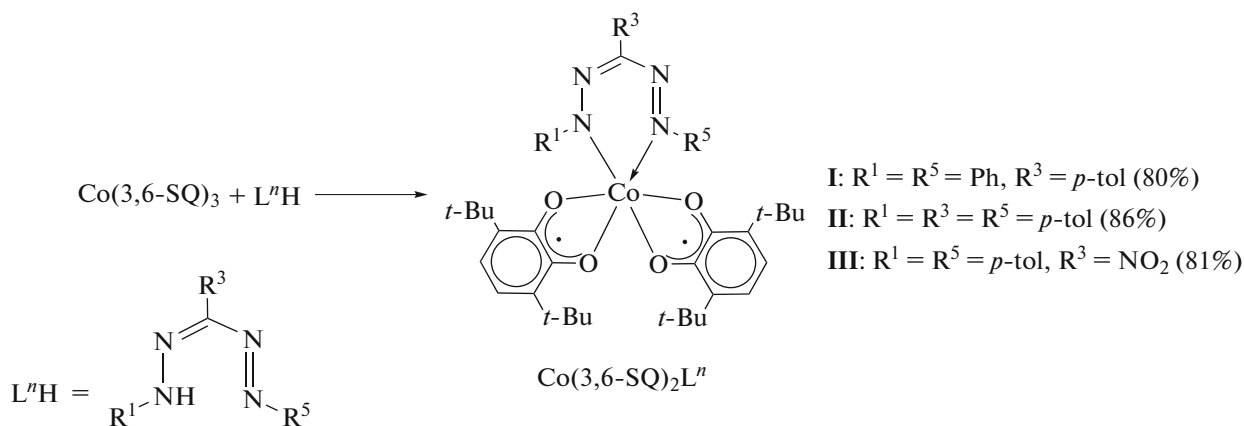
The full set of XRD parameters was deposited with the Cambridge Crystallographic Data Centre (CIF files CCDC nos. 2161722 (**I**), 2167094 (**II**), and 2167095 (**III**); <https://www.ccdc.cam.ac.uk/structures/>).

RESULTS AND DISCUSSION

The exchange reaction between metal tris-*o*-semiquinolate and neutral ligand is the general method for the synthesis of heteroligand *o*-semiquinone complexes of transition metals [42, 43]. Using this method we synthesized new heteroligand hexacoordinate cobalt(III) bis-*o*-semiquinoneformazanate complexes shown in Scheme 1. Synthesized complexes **I–III** in the crystalline state are resistant to air oxygen and moisture and highly soluble in the most part of organic solvents.

Table 2. Selected bond lengths (Å) and angles (deg) in complexes I–III

Bond	I	II	III
	<i>d</i> , Å		
Co(1)–O(1)	1.922(3)	1.9007(16)	1.8915(14)
Co(1)–O(2)	1.894(3)	1.9082(17)	1.9120(14)
Co(1)–O(3)	1.906(3)	1.9360(19)	1.9064(14)
Co(1)–O(4)	1.889(3)	1.8674(17)	1.8731(14)
Co(1)–N(1)	1.899(4)	1.9282(19)	1.9246(17)
Co(1)–N(4)	1.892(4)	1.913(2)	1.9078(17)
O(1)–C(1)	1.298(5)	1.291(3)	1.292(2)
O(2)–C(2)	1.312(5)	1.300(3)	1.304(2)
O(3)–C(15)	1.304(6)	1.293(3)	1.290(2)
O(4)–C(16)	1.303(6)	1.296(3)	1.302(2)
N(1)–N(2)	1.296(5)	1.288(3)	1.279(2)
N(2)–C(35)	1.348(6)	1.348(3)	1.331(3)
N(3)–C(35)	1.355(6)	1.328(3)	1.333(3)
N(3)–N(4)	1.284(5)	1.297(3)	1.277(2)
Angle	I	II	III
	ω , deg		
O(1)–Co(1)–O(2)	85.07(13)	84.28(7)	84.93(6)
O(3)–Co(1)–O(4)	85.27(14)	84.50(8)	86.06(6)
N(1)–Co(1)–N(4)	85.77(17)	86.00(9)	87.95(7)
N(1)–Co(1)–O(1)	177.82(16)	178.12(8)	174.26(7)
O(2)–Co(1)–O(4)	172.32(16)	170.86(7)	169.71(6)
O(3)–Co(1)–N(4)	175.92(16)	171.20(9)	173.07(7)

**Scheme 1.**

The IR spectra of compounds I–III are characterized by a set of vibration bands of the ligands composing the complex. The IR spectrum of the compounds contains intense bands of stretching vibrations of the sesquialteral C–O bonds of the *o*-semiquinone ligands (1350–1450 cm^{-1}) and medium-intensity bands cor-

responding to stretching vibrations of the C=N and N=N bonds of the coordinated formazanate ligands (1610–1540 cm^{-1}).

According to the XRD data, compounds I and III crystallize in the monoclinic space group $P2_1/c$, unlike complex II, which crystallizes in the triclinic space

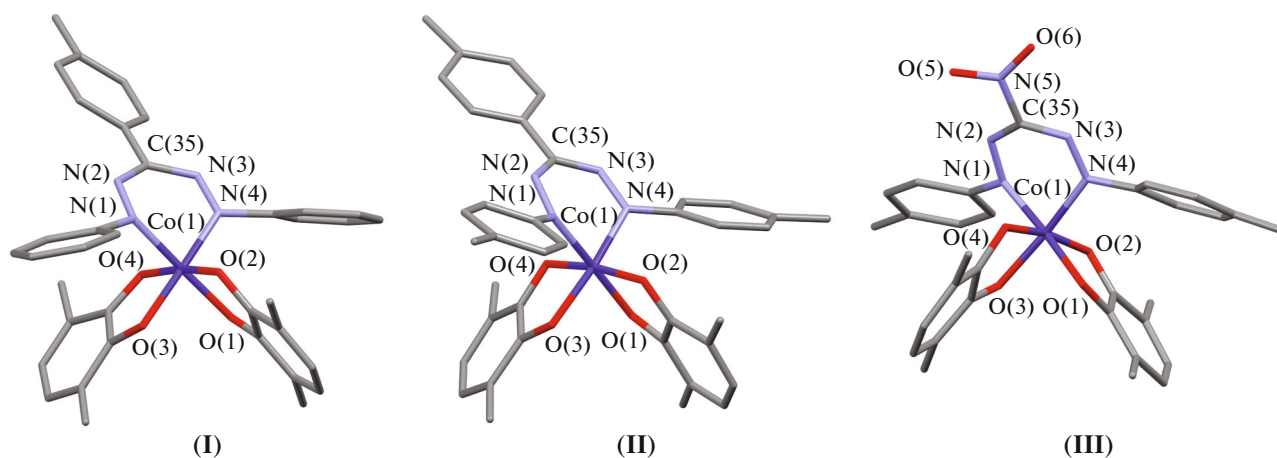


Fig. 1. Molecular structures of complexes **I**, **II**, and **III** according to the XRD data. Methyls of *tert*-butyl groups and hydrogen atoms are omitted.

group $P\bar{1}$. In each molecule, the central cobalt atom exists in the octahedral environment (Fig. 1). The Co–O (1.8674(17)–1.9360(19) Å) and Co–N (1.892(4)–1.9282(19) Å) bond lengths lie in a range characteristic of the hexacoordinate complexes of low-spin cobalt(III) [44, 45]. The C–O and C–C bond lengths inside the O,O'-chelating quinone ligands are typical of the radical anion *o*-benzosemiquinone form [46, 47]. The bond length distribution inside the formazanate fragment N(1)N(2)C(35)N(3)N(4) indicates the anionic form of the ligand [48, 49]. The chelate formazanate metalocycle is nonplanar and bent along the N(1)...N(4) line. In addition, the *meso*-C(35) carbon atom deviates from the N(1)N(2)N(3)N(4) plane. The largest bending angle of the metalocycle (38.13°) and the highest deviation of the C(35) carbon atom (0.158 Å) are observed for compound **II** with the most bulky substituents in the formazanate ligand. These parameters for compound **I** are 34.95° and 0.154 Å, and for compound **III** they are 33.08° and 0.140 Å, respectively. In complex **I**, the phenyl substituents at the N(1) and N(4) nitrogen atoms of the formazan ligand are turned relatively to the azohydrazone plane by an angle of ~50°. An asymmetry in the arrangement of these substituents is observed for compounds **II** and **III**: 37° and 27° in **II**, and 35° and 43° in **III**. This distinction is related, most likely, to differences in crystal packings of the complexes. The crystals of complex **I** exhibit a similar packing motif described previously for cobalt(III) bis-*o*-semiquinonates with 1-aryl-3,5-diphenylformazan ligands [24]: molecules of the complexes are packed in skewed stacks in such a way that the paramagnetic *o*-semiquinone ligands of the adjacent stacks are directed to each other and parallel (Fig. 2). The distance between the *o*-semiquinone ligands of the adjacent stacks is 4.651 Å for complex **I**. The packing mode for compounds **II** and **III** differs from the described one: in this case, parallel stacks of

molecules of the complexes are directed to each other by the formazanate fragments, which results in the mutual repulsion of the substituents at the N(1) and N(4) atoms between the adjacent molecules and, as a consequence, in an asymmetry in the arrangement of these substituents (Figs. 3, 4). The distance between the N(1)N(2)N(3)N(4) planes of the adjacent formazanate fragments is 4.856 and 4.595 Å for compounds **II** and **III**, respectively. Intermolecular contacts of the nitro groups with the hydrogen atoms of the *p*-tolyl (*p*-Tol) and *tert*-butyl (*t*-Bu) substituents (Fig. 4) are observed in the crystal of complex **III**. The lengths of the O...H(*p*-Tol) and N...H(*t*-Bu) contacts are 2.456 and 2.666 Å, which corresponds to the usual van der Waals interactions O...H and N...H (2.45 and 2.64 Å, respectively [50]). The intermolecular shortened van der Waals C...H and H...H contacts (<2.82 and 2.31 Å [50]) were found between the *t*-Bu substituents in stacks of molecules of complex **III** along the *c* axis. The lengths of the C...H and H...H contacts are 2.732 and 2.192 Å, respectively.

The magnetic properties of complexes **I–III** in a temperature range of 2–300 K were studied. The temperature dependences of μ_{eff} for these complexes are shown in Fig. 5. The magnetic behavior of complex **I** differs insignificantly from that of analogous cobalt(III) bis-*o*-semiquinone complex with the unsubstituted 1,3,5-triphenylformazan ligand [23]. The high-temperature value of μ_{eff} for compound **I** is 2.52 μ_{B} , which is close to a spin-only value of 2.45 μ_{B} calculated for the system of two radical centers with $S = 1/2$ for each center. This state of the system corresponds to the Co(III) complex bound to two radical anion *o*-semiquinone ligands and one formazanate anion. With decreasing temperature, the magnetic moment first decreases smoothly in a range of 300–100 K and then decreases more sharply to 0.34 μ_{B} at 2 K indicating the antiferromagnetic character of

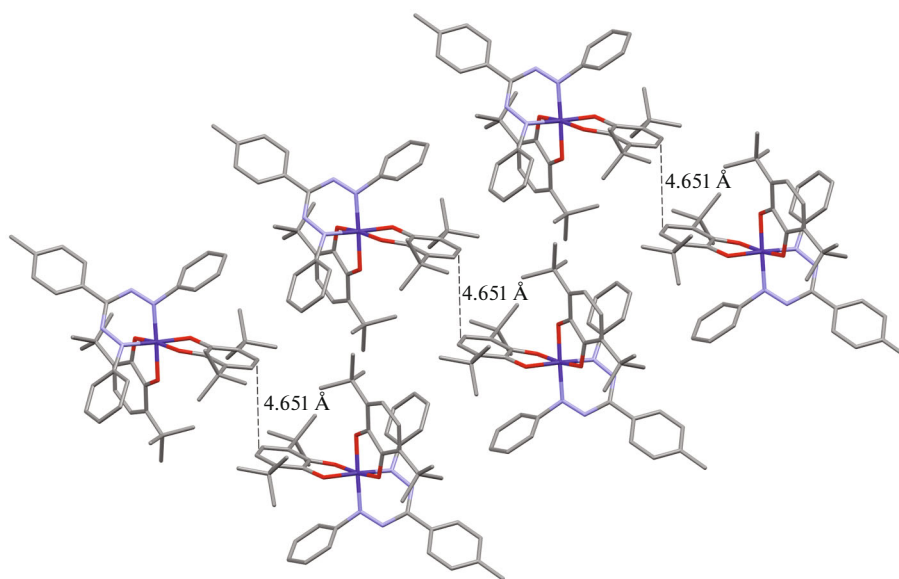


Fig. 2. Fragment of the crystal packing of complex I. Hydrogen atoms are omitted.

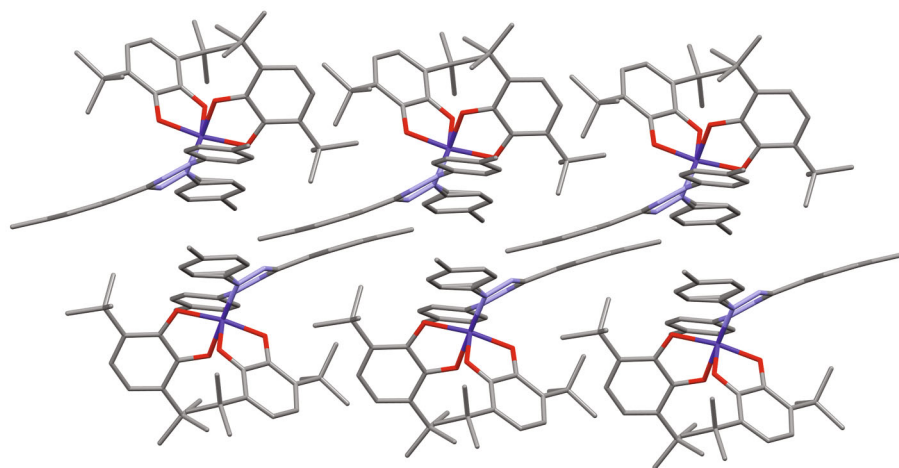


Fig. 3. Fragment of the crystal packing of complex II. Hydrogen atoms are omitted.

exchange between the radical centers. The high-temperature value of μ_{eff} for complexes **II** and **III** (1.93 and 1.33 μ_{B} , respectively) is appreciably lower than the value expected for the spin system of two radical centers with $S = 1/2$. With decreasing temperature, μ_{eff} of these complexes decreases smoothly and at 5 K reaches 0.11 μ_{B} and 0.45 μ_{B} for complexes **II** and **III**, respectively. We examined the experimental dependences $\mu_{\text{eff}}(T)$ using the exchange-coupled dimer model ($H = -2JS_1S_2$). The optimum values of the exchange interaction parameter J and g factor are given in Table 3. For clarity, the table was supplemented by analogous parameters for the earlier described cobalt(III) bis-*o*-semiquinolate complexes with phenyl substituents in the first and fifth positions

of the formazanate ligand. The data in Table 3 show that the replacement of the phenyl substituents by *p*-tolyl substituents in the first and fifth positions of the formazanate ligand in the series of the complexes of the general type $\text{Co}(3,6\text{-SQ})_2\text{L}'$ results in a considerable enhancement of the exchange between the radical centers, and the exchange type remains unchanged, viz., antiferromagnetic. The maximum exchange parameter is observed for complex **III**. We believe that the exchange enhancement observed between the radical centers is related to the fact that the angle between the *o*-semiquinone ligands decreases upon the replacement of the phenyl substituents in positions 1 and 5 of the formazanate ligand by *p*-tolyl substituents in the crystal structures of the

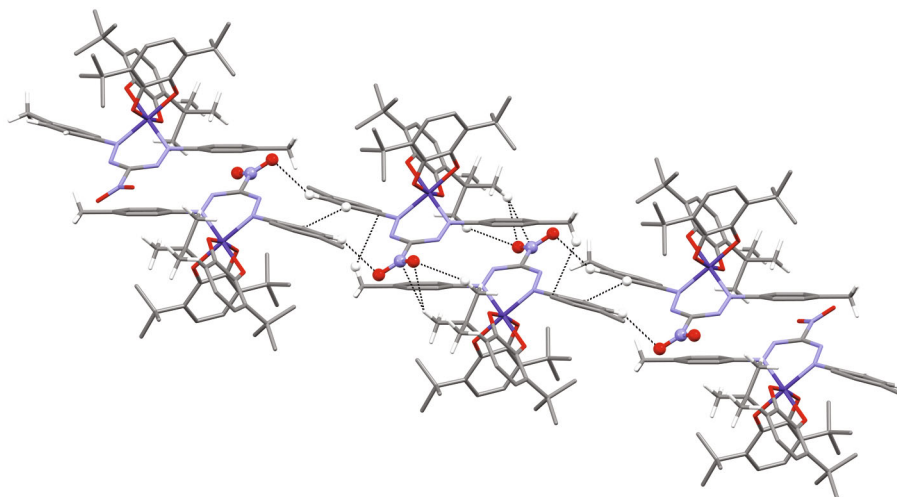


Fig. 4. Fragment of the crystal packing of complex III.

$\text{Co}(3,6\text{-SQ})_2\text{L}^n$ complexes. For example, this angle is 75.94° in the complex with 1,3,5-triphenylformazan [23], the angle is 76.16° in compound I with 1,5-diphenyl-3-*p*-tolylformazan, and these angles are 66.87° and 68.11° in compounds II and III with 1,5-di-*p*-tolyl-substituted formazans, respectively. In the case of complex III, the value of exchange is likely affected simultaneously by two factors: a decrease in the angle between the radical anion ligands and the presence of the electron-acceptor nitro group in the third position of the formazanate ligand.

Thus, the insertion of a *p*-tolyl substituent in the third position of the formazanate ligand exerts no substantial effect on the magnetic behavior of the heteroligand cobalt(III) *o*-semiquinoneformazanate complexes, whereas the insertion of *p*-tolyl substituents in

the first and fifth positions of the formazanate ligand changed the geometry of the complex and significantly enhanced the exchange between the radical *o*-semiquinone ligands.

ACKNOWLEDGMENTS

Elemental analysis and IR spectroscopy of compounds I–III and XRD studies of complexes II and III were carried out using the equipment of the Center for Collective Use “Analytical Center of Institute of Organometallic Chemistry of Russian Academy of Sciences” at the Razuvaev Institute of Organometallic Chemistry (Russian Academy of Sciences) supported by the project “Provision of Development of Material Technical Infrastructure of Centers for

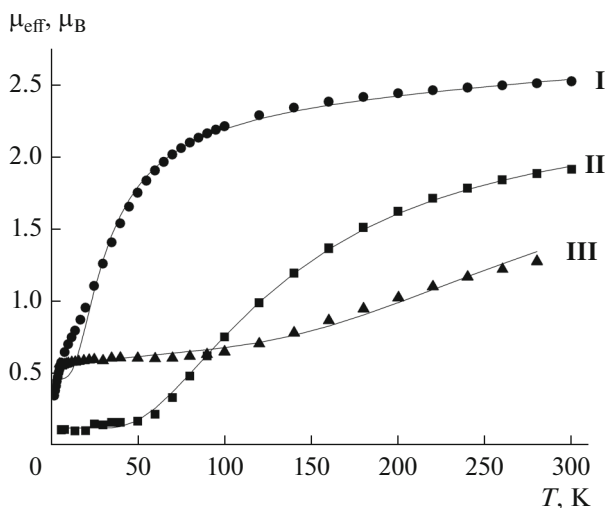


Fig. 5. Temperature dependences of the effective magnetic moments for complexes (●) I, (■) II, and (▲) III (solid lines are theoretical curves).

Table 3. Approximation results for the magnetic properties of complexes $\text{Co}(3,6\text{-SQ})_2\text{L}^n$

Parameter	$\text{R}^1 = \text{R}^5 = \text{Ph}$			$\text{R}^1 = \text{R}^5 = p\text{-Tol}$	
	$\text{R}^3 = \text{Ph}$ [23]	$\text{R}^3 = p\text{-Tol}$ (I)	$\text{R}^3 = \text{NO}_2$ [25]	$\text{R}^3 = p\text{-Tol}$ (II)	$\text{R}^3 = \text{NO}_2$ (III)
$J_{\text{SQSQ}}, \text{K}$	-65.4 (0.4)	-38.8 (0.7)	-187.2 (0.4)	-185.6 (0.7)	-404.7 (8.9)
$g(\text{SQ})$	2.04 (0.01)	2.00 (0)	2.00 (0)	2.00 (0)	2.00 (0)

Collective Use of Scientific Equipment” (RF-2296.61321X0017).

FUNDING

This work was supported by the Russian Science Foundation, project no. 20-73-00157.

CONFLICT OF INTEREST

The authors declare that they have no conflicts of interest.

REFERENCES

- Lipunova, G.N., Fedorchenko, T.G., and Chupakhin, O.N., *Russ. J. Gen. Chem.*, 2019, vol. 89, no. 6, p. 1225.
- Gilroy, J.B. and Otten, E., *Chem. Soc. Rev.*, 2020, vol. 49, p. 85.
- Kamphuis, A.J., Milocco, F., Koiter, L., et al., *ChemSusChem*, 2019, vol. 12, p. 3635.
- Broere, D.L.J., Mercado, B.Q., and Holland, P.L., *Angew. Chem.*, 2018, vol. 130, p. 6617.
- Travieso-Puente, R., Broekman, J.O.P., Chang, M.-C., et al., *J. Am. Chem. Soc.*, 2016, vol. 138, p. 5503.
- Milocco, F., de Vriers, F., Bartels, I.M.A., et al., *J. Am. Chem. Soc.*, 2020, vol. 142, p. 20170.
- Milocco, F., de Vriers, F., Siebe, H.S., et al., *Inorg. Chem.*, 2021, vol. 60, p. 2045.
- Maar, R.R., Barbon, S.M., Sharma, N., et al., *Chem. Eur. J.*, 2015, vol. 21, p. 15589.
- Barbon, S.M., Novoa, S., Bender, D., et al., *Org. Chem. Front.*, 2017, vol. 4, p. 178.
- Hesari, M., Barbon, S.M., Staroverov, V.N., et al., *ChemComm*, 2015, vol. 51, p. 3766.
- Hesari, M., Barbon, S.M., Mendes, R.B., et al., *J. Phys. Chem. C*, 2018, vol. 122, p. 1258.
- Novoa, S. and Gilroy, J.B., *Polym. Chem.*, 2017, vol. 8, p. 5388.
- Dhindsa, J.S., Maar, R.R., Barbon, S.M., et al., *ChemComm*, 2018, vol. 54, p. 6899.
- Mandal, A., Schwederski, B., Fiedler, J., et al., *Inorg. Chem.*, 2015, vol. 54, p. 8126.
- Milocco, F., Demeshko, S., Meyer, F., et al., *Dalton Trans.*, 2018, vol. 47, p. 8817.
- Broere, D.L.J., Mercado, B.Q., Lukens, J.T., et al., *Chem. - Eur. J.*, 2018, vol. 24, p. 9417.
- Broere, D.L.J., Mercado, B.Q., Bill, E., et al., *Inorg. Chem.*, 2018, vol. 57, p. 9580.
- Kabir, E., Patel, D., Clark, K., et al., *Inorg. Chem.*, 2018, vol. 57, p. 10906.
- Mu, G., Jiang, C., and Teets, T.S., *Chem. - Eur. J.*, 2020, vol. 26, p. 11877.
- Protasenko, N.A. and Poddel'sky, A.I., *Theor. Exp. Chem.*, 2020, vol. 56, p. 338.
- Bellan, E.V., Poddel'sky, A.I., Protasenko, N.A., et al., *Inorg. Chem. Commun.*, 2014, vol. 50, p. 1.
- Protasenko, N.A., Poddel'sky, A.I., Bogomyakov, A.S., et al., *Polyhedron*, 2013, vol. 49, p. 239.
- Protasenko, N.A., Poddel'sky, A.I., Bogomyakov, A.S., et al., *Inorg. Chem.*, 2015, vol. 54, p. 6078.
- Protasenko, N.A., Poddelskii, A.I., Rumyantsev, R.V., et al., *Russ. J. Coord. Chem.*, 2021, vol. 47, p. 687. <https://doi.org/10.1134/S1070328421100067>
- Protasenko, N.A., Arsenyev, M.V., Baranov, E.V., et al., *Eur. J. Inorg. Chem.*, 2022. <https://doi.org/10.1002/ejic.202200152>
- Belostotskaya, I.S., Komissarova, N.L., Dzhuraryan, Z.V., et al., *Izv. Akad. Nauk SSSR. Ser. Khim.*, 1972, no. 7, p. 1594.
- Ashley, J.N., Davis, B.M., Nineham, A.W., et al., *J. Chem. Soc.*, 1953, p. 3881.
- von Eschwege, K.G., *J. Photochem. Photobiol., A*, 2013, vol. 252, p. 159.
- Lange, C.W., Couklin, B.J., and Pierpont, C.G., *Inorg. Chem.*, 1994, vol. 33, p. 1276.
- Gordon, A.J. and Ford, R.A., *The Chemist's Companion*, New York: Wiley, 1972.
- APEX3. SAINT and SADABS, Madison: Bruker AXS Inc., 2016.
- Sheldrick, G.M., *Acta Crystallogr., Sect. A: Found. Adv.*, 2015, vol. 71, p. 3.
- Sheldrick, G.M., *Acta Crystallogr., Sect. C: Cryst. Chem.*, 2015, vol. 71, p. 3.
- Dolomanov, O.V., Bourhis, L.J., Gildea, R.J., et al., *J. Appl. Crystallogr.*, 2009, vol. 42, p. 339.
- CrysAlisPro 1.171.38.46. Data Collection, Reduction and Correction Program. Software Package, Rigaku OD, 2015.
- APEX3. Version 2018.7-2. Bruker Molecular Analysis Research Tool, Madison: Bruker AXS Inc., 2018.
- SAINT. Version 8.38A. Data Reduction and Correction Program, Madison: Bruker AXS Inc., 2017.
- Krause, L., Herbst-Irmer, R., Sheldrick, G.M., and Stalke, D., *J. Appl. Crystallogr.*, 2015, vol. 48, p. 3.
- Sheldrick, G.M. SHELXTL. Version 6.14. Structure Determination Software Suite, Madison: Bruker AXS, 2003.

40. SCALE3 ABSPACK: Empirical Absorption Correction. *CrysAlisPro 1.171.38.46, Software Package*, Rigaku OD, 2015.
41. Sheldrick, G.M., *SADABS. Version 2016/2. Bruker/Siemens Area Detector Absorption Correction Program*, Madison: Bruker AXS Inc., 2016.
42. Pierpont, C.G. and Buchanan, M.N., *Coord. Chem. Rev.*, 1981, vol. 38, p. 45.
43. Abakumov, G.A., Lobanov, A.V., Cherkasov, V.K., et al., *Inorg. Chim. Acta*, 1981, vol. 49, p. 135.
44. Lange, C.W., Couklin, B.J., and Pierpont, C.G., *Inorg. Chem.*, 1994, vol. 33, p. 1276.
45. Dai, J., Kanegawa, S., Li, Z., et al., *Eur. J. Inorg. Chem.*, 2013, p. 4150.
46. Brown, S.N., *Inorg. Chem.*, 2012, vol. 51, no. 3, p. 1251.
47. Pavlova, N.A., Poddel'sky, A.I., Bogomyakov, A.S., et al., *Inorg. Chem. Commun.*, 2011, vol. 14, no. 10, p. 1661.
48. Gilroy, J.B., Ferguson, M.J., McDonald, R., et al., *Chem. Commun.*, 2007, p. 126.
49. Chang, M.-Ch., Dann, T., Day, D.P., et al., *Angew. Chem., Int. Ed. Engl.*, 2014, vol. 53, p. 4118.
50. Zefirov, Yu. V. and Zorkii, P.M., *Usp. Khim.*, 1995, vol. 64, no. 5, p. 446.

Translated by E. Yablonskaya